Progress In Electromagnetics Research C, Vol. 73, 47–53, 2017

Additive Manufactured Double-Ridged Horn Antenna for UWB Applications

Diego Betancourt[1, *], Klaus Wolf[2], Dirk Plettemeier[2], and Frank Ellinger[1]

Abstract—In this paper, the design, fabrication, and test of an additive manufactured double-ridged horn antenna optimized to work in ultra-wide-band frequencies is introduced. In particular, to build this antenna, the fused deposition modeling fabrication method is selected. The plastic-made device is then coated by using conductive ink. The double-ridged horn is conceived as a monolithic block. In this way, performance degradations caused by fabrication inaccuracies are minimized. A very good agreement between the simulations and the antenna measurements is demonstrated. The proof-of-concept prototype has an outstanding operational bandwidth performance of 11.5 GHz (fc 8.25 GHz) with a gain of 6 dBi; its total weight is less than 200 gr, and the total prototyping fabrication costs are less than 10 Euro per antenna with a lead time of less than a week.

1. INTRODUCTION

Modern communications systems and high-frequency RF applications requiring broad bandwidth normally use a horn antenna as a suitable solution for very demanding performance applications. Compared to another type of antennas, the horn has more directivity, has more gain with low side-lobes and can support high power sources, as well. However, despite high-performance characteristics, horn and double-ridged horn antennas (DRHA), may suffer from several fabrication-related drawbacks, e.g., heavyweight, complex fabrication processes, high manufacturing prices and long lead times.

In this regard, the additive manufacturing (AM) technology has recently been introduced as a viable alternative to produce high-performance passive RF components. With the AM technology, it is possible to create high-complexity 3D structures in a monolithic block with a very high aspect ratio at very competitive prices and achieving similar performances as with the traditional fabrication methods. Thus, this novel and revolutionary manufacturing technology can help to overcome some of the aforementioned open issues related to the fabrication of a DRHA.

In the literature, few AM built horn antennas have been reported so far [1–4]. All these antennas use stereolithography apparatus (SLA) method to be fabricated instead fused deposition modeling (FDM) as is in this work reported. A simple low-cost mobile ground terminal antenna for Ka-band satellite communications (18 to 32 GHz) is presented in the work of Silva et al. [1]. An interesting approach to the fabrication of millimeter-wave corrugated Horn antennas in the 75 to 110 GHz frequency band is shown in the paper of Timbie et al. [2] although this antenna is not conceived as a monolithic block. Two different compact high gain antennas working at Ku band (12 to 18 GHz) frequency range, were designed, built and tested for spatial applications as is reported in the work of Van der Vorst and Gumpinger [3]. A remarkable result is reported by Bieren et al. [4]. In that work, a diagonal horn antenna for the WR-3.4 band (220–330 GHz) is manufactured and characterized. The work of Viera et al. [5] describes the development of a horn antenna working from 8 to 18 GHz by using the FDM

Received 14 February 2017, Accepted 27 March 2017, Scheduled 6 April 2017

* Corresponding author: Diego Betancourt (diego.betancourt@tu-dresden.de).

[1] Circuit Design and Network Theory, TU Dresden, Dresden, D-01069, Germany. [2] Radio frequency and Photonics Engineering, TU Dresden, Dresden, D-01069, Germany.

fabrication method and different metallization techniques, although this antenna is not conceived as a monolithic block and cannot be fed by a coax cable.

In this paper, the design, fabrication, and test of an AM DRHA are introduced. To build the antenna, the FDM fabrication method and a polymer material are selected. After manufacturing the antenna, it is coated using a conductive ink based on silver. The antenna is optimized to work in UWB frequencies, specifically between 2.5 to 14 GHz. A very good agreement between simulations and measurements of the fabricated antenna is demonstrated. The antenna is conceived as a monolithic block, and in this way, the lack of performance caused by the fabrication inaccuracies are minimized. The proof-of-concept prototype has an outstanding operational bandwidth performance of 11.5 GHz (fc 8.25 GHz) with a gain of 6 dBi; its total weight is less than 200 gr, and the total fabrication cost sum less than 10 Euro per unit with a lead time of less than a week.

2. ANTENNA DESIGN AND SIMULATION

The antenna design requirements include a bandwidth covering the whole UWB frequency band from 3.1 to 10.6 GHz (i.e., a fractional bandwidth close to 100%), a compact size, a light-weighted device and connectivity through SMA connectors. In view of those requirements, a DRHA is selected to be designed due to inherent large bandwidth capabilities which match with the expected application. This kind of antenna is widely known and has demonstrated to have a large bandwidth, good impedance characteristics and exceptional gain at different frequency bands [6, 7].

An interesting point, regarding a DRHA, is the elevated manufacturing difficulty which is not suitable for monolithic process fabrication when conventional methods, as milling and similar, are used. Normally, a DRHA is fabricated by splitting the design into spare components that are assembled afterward [2, 6, 7]. In this regard, the using of AM techniques allow to the manufacturing of such complex structures as a simple monolithic block reducing by this way, the performance errors introduced by assembling misalignments and by fabrication tolerances.

A DRHA contains four main sub-sections: the feeding section, the waveguide and the back cavity section, the ridged flanges section and the pyramidal part. A perspective view and a cutaway view of a DRHA are shown in Fig. 1.

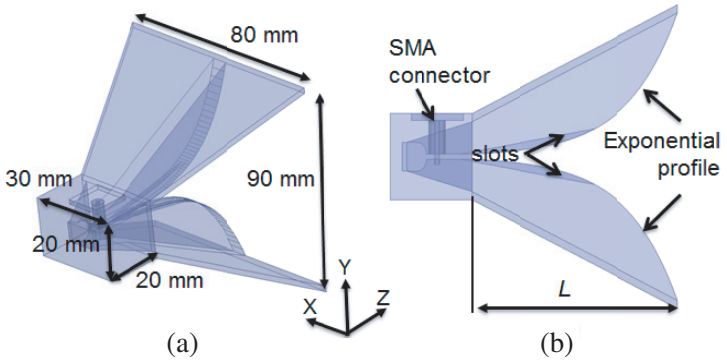

Figure 1. (a) Perspective view of a DRHA and (b) cutaway view.

The antenna feeding is an SMA coaxial connector. The feed guides the energy through the upper ridge into the gap between the ridges in a way that the outer conductor is connected to the upper ridge and the inner conductor connects to the lower one. The inner connector diameter is 1 mm and the outer diameter is appx. 5 mm filled with TFE-Fluorocarbon. For the concept demonstrator antenna, a commercial SMA connector with extended insulation from TE-Connectivity with reference 1052523-1 was selected.

The double-ridged waveguide is widely used in antenna design as a way to increase the antenna bandwidth and to improve the impedance characteristics [8]. The design parameters of this component are based on the waveguide and ridge dimensions ($a1$, $a2$, $b1$ and $b2$) as are shown in Fig. 2. For the dimensions, some general design guidelines are available in the literature [8, 9], or can be achieved from

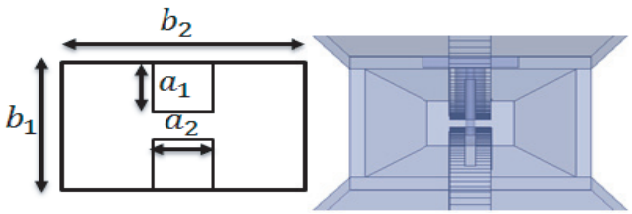

Figure 2. Double ridged waveguide schematic and parameters. On the left-hand side, the double ridged waveguide and definition of dimension parameters ($a1 = 9.4\,\text{mm}$, $a2 = 6\,\text{mm}$, $b1 = 20\,\text{mm}$ and $b2 = 30\,\text{mm}$) and, on the right-hand side, a detailed design view.

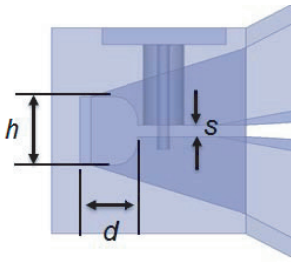

Figure 3. A cutaway view of the back cavity. With $h = 7\text{mm}$, $d = 7\,\text{mm}$, and $s = 1.2\,\text{mm}$.

commercial products [6, 7]. The only design restriction applying here is on the wide of the ridge ($a2$) which must be enough wide as to allocate a standard coaxial feeder (as the one selected for our antenna which has a diameter of appx. 5 mm). In order to improve the antenna performance, the design values alongside with the whole antenna dimensions are optimized by using an EM CAD software.

The cavity section plays an important role for the matching of the waveguide to the coaxial cable which feeds the antenna. The optimal dimensions, h and d, are obtained through the analysis of the S_{11} parameter under the condition of $-10\,\text{dB}$ for the working frequency band. With the purpose of easy the fabrication process, the cavity's corners are rounded. The transition of this cavity to the waveguide box is done by four triangular shaped flaps on the four walls of the waveguide which forms a conical structure. The final aspect of the back cavity is shown in Figs. 2 and 3.

The horn aperture dimensions are $80\,\text{mm} \times 90\,\text{mm}$, and the TEM section axial length $L = 60\,\text{mm}$. Here, the function of the ridges is to provide a smooth transition from the waveguide impedance to the free-space impedance ($370\,\Omega$). Different types of ridges profiles, such as exponential, sinusoidal and binomial have been employed so far, but it has been mentioned in the literature that the exponential profile offers the best match between the impedance of the waveguide section and free-space. Hence, the selected profile of the ridge section follows the exponential-like equation $y(z) = \frac{s}{2}e^{zk}$ $0 \leq z \leq L$, with $k = \frac{1}{L}\ln(\frac{Y_{ap}}{s})$, where the horn aperture distance $Y_{ap} = 90\,\text{mm}$ and the gap between the ridges in the feeding waveguide (s) is equal to 1.2 mm. This distance, s, is dependent to the fabrication tolerances and although smaller values could give better results, in terms of S_{11} and VSWR, the accuracy of the fabrication technique determines the minimum value achievable without fabrication errors, which is selected to be 1.2 mm (for FDM).

In order to improve the impedance characteristic of the antenna, the ridges include a slot as proposed in [10]. The appearance and dimensions of such slots are shown in the Fig. 1. The slots also help to demonstrate the fabrication procedure versatility, which can reproduce complex singularities without additional effort.

To make a transition from the waveguide section to the free-space, four flared walls are required, as in a normal horn antenna configuration can be observed. However, due to the high concentration of the electrical energy between the ridges, especially at the higher frequencies, the lateral side walls have a negligible effect on the performance of the antenna [11]. For this reason, these side flares are suppressed from the antenna design without attempting to the throughput of the same.

Time domain full wave electromagnetic simulations and parametric optimization were conducted for the antenna modeling. For this purpose, we have worked with the Ansys-HFSS simulator. The optimization includes all antenna parameters but in special those related to the back cavity and waveguide dimensions. The optimization is conducted in a way to achieve an S_{11} response below $-10\,\text{dB}$ in the UWB frequency range.

3. FABRICATION PROCEDURE

For the fabrication of the DRHA, an AM technique was selected. In particular, the fused deposition modeling technology was used. The FDM is an AM technology commonly used for modeling, prototyping, and production applications. It is one of the techniques used for 3D printing. FDM works on an "additive" principle by laying down material in layers; a plastic filament is unwound from a coil and supplies material to produce a part. The molten material is forced out of the print head's nozzle and is deposited on the growing workpiece. The head is moved, under computer control, to define the printed shape. Usually, the head moves in layers, moving in two dimensions to deposit one horizontal plane at a time, before moving slightly upwards to begin a new slice. The speed of the extruder head may also be controlled, to stop and start deposition and form an interrupted plane without stringing or dribbling between sections.

To fabricate the antenna, a MakerBot Replicator FDM machine from Stratasys with a polymer filament of 1.75 mm diameter was used [12]. The fabricated aspect of the antenna before the coating is shown in Fig. 4. The manufactured antenna weighs less than 200 gr. In order to add the EM properties to the antenna, this must be metalized. The metallization procedure can be done by using different techniques such as galvanization, metal-evaporation, and coating. The fabricated antenna was coated by painting it with a conductive ink (silver-based ink). In particular, a nano-silver particles ink in a suspension of Methyl-Isobutyl-Ketone from Holland Shielding Systems BV was used. This ink offers a good conductivity while a minimum resistance per square meter is observed (sheet resistance < 0.015/square). Two painting layers were used to coat the antenna. The conductivity of the resultant surface was verified by using a multi-meter. The results obtained in this initial test suggest that the coating confers to the antenna the metallic characteristics to allow the EM phenomenon to occur.

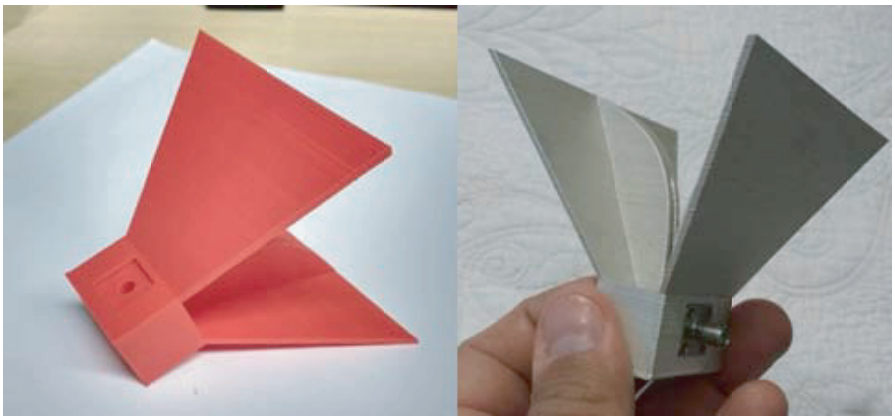

Figure 4. Actual aspect of the DRHA before and after being coated with silver ink.

The thickness of the applied layers accounts for a couple of μm, but it was not experimental measured. Nevertheless, at the working frequencies (2 to 14 GHz) the skin depth is large enough when compared to the coating thickness and hence any degradation on the antenna's performance, for this reason, is expected.

Another important parameter, to be taken into account, is the antenna surface roughness. As can be observed from Fig. 4, the roughness of the elaborated antenna is large enough to be noted with a naked eye. This roughness corresponds to the fabrication accuracy of the FDM fabrication method and might be the cause of performance mismatches of the antenna.

4. EXPERIMENTAL RESULTS

The return loss parameter of the DRHA was measured using a vector network analyzer from Anrtitsu. A total of 1600 points in frequency were measured. The S_{11} experimental results are shown in Fig. 5.

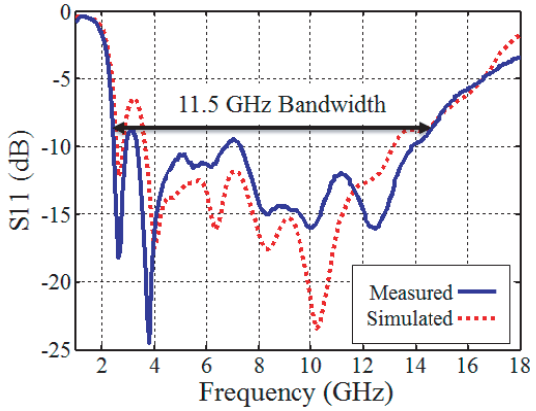

Figure 5. Return loss parameter of the AM DRHA.

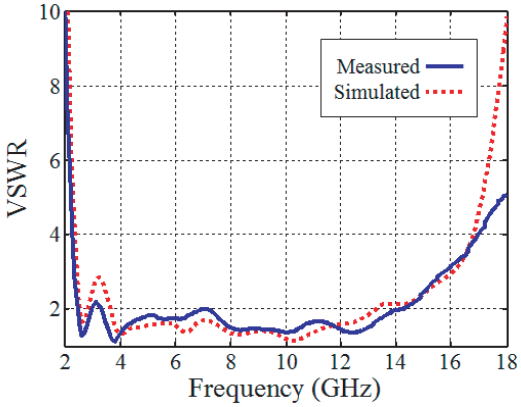

Figure 6. VSWR of the AM DRHA.

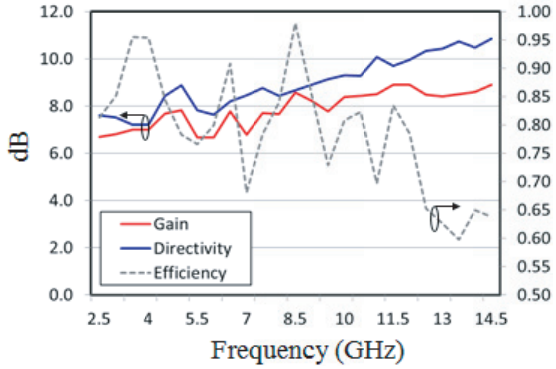

Figure 7. Measured gain, directivity and efficiency of the AM DRHA.

From the figure, a good agreement between the simulation and measurement results can be observed. Such good results are a direct consequence of the DRHA's concept and manufacturing as a monolithic block avoiding misalignment errors due to the assembling of several pieces. The only spare component is the SMA connector, which alongside the surface roughness have been identified as the main source of errors for the antenna behavior.

A notable deviation on measurement at 3 GHz is observed. At this frequency, a poor S_{11} response was expected due to the ridge separation (s) in the waveguide which is set to 1.2 mm but, as a consequence of the fabrication accuracy, this separation is narrowed leading an improvement in this parameter (at 3 GHz). As a result, the overall operational antenna bandwidth is extended. The operational bandwidth of the DRHA is measured to occupy 11.5 GHz (@ −9 dB) from 2.5 GHz to 14 GHz, with a fractional bandwidth of 140% (with fc 8.25 GHz). This result suggests that the silver-ink coated AM antenna works as expected.

Another parameter used to verify the behavior of the DRHA is the voltage standing wave ratio (VSWR). In the Fig. 6 the good agreement between measurement and simulations is observed. A VSWR of less than 2 for an 11.5 GHz bandwidth (2.5 to 14 GHz) is obtained.

Additionally, the gain was measured. For this purpose, the comparison method with a reference antenna was applied. The resulting gain, as well as the estimated directivity of the antenna, is shown in Fig. 7. Using the results shown in the same figure, the averaged efficiency of the antenna was calculated to be near to 0.8 for all the working bandwidth.

In order to verify the real behavior of the designed antenna, several radiation patterns were measured. The measurement setup takes place in an anechoic chamber and a near-field setup was used. In particular, a spherical near-field scanner equipment from NSI model 700-30 was used. The observation window goes from −180 to 180 deg. in azimuth and elevation with an angular resolution of

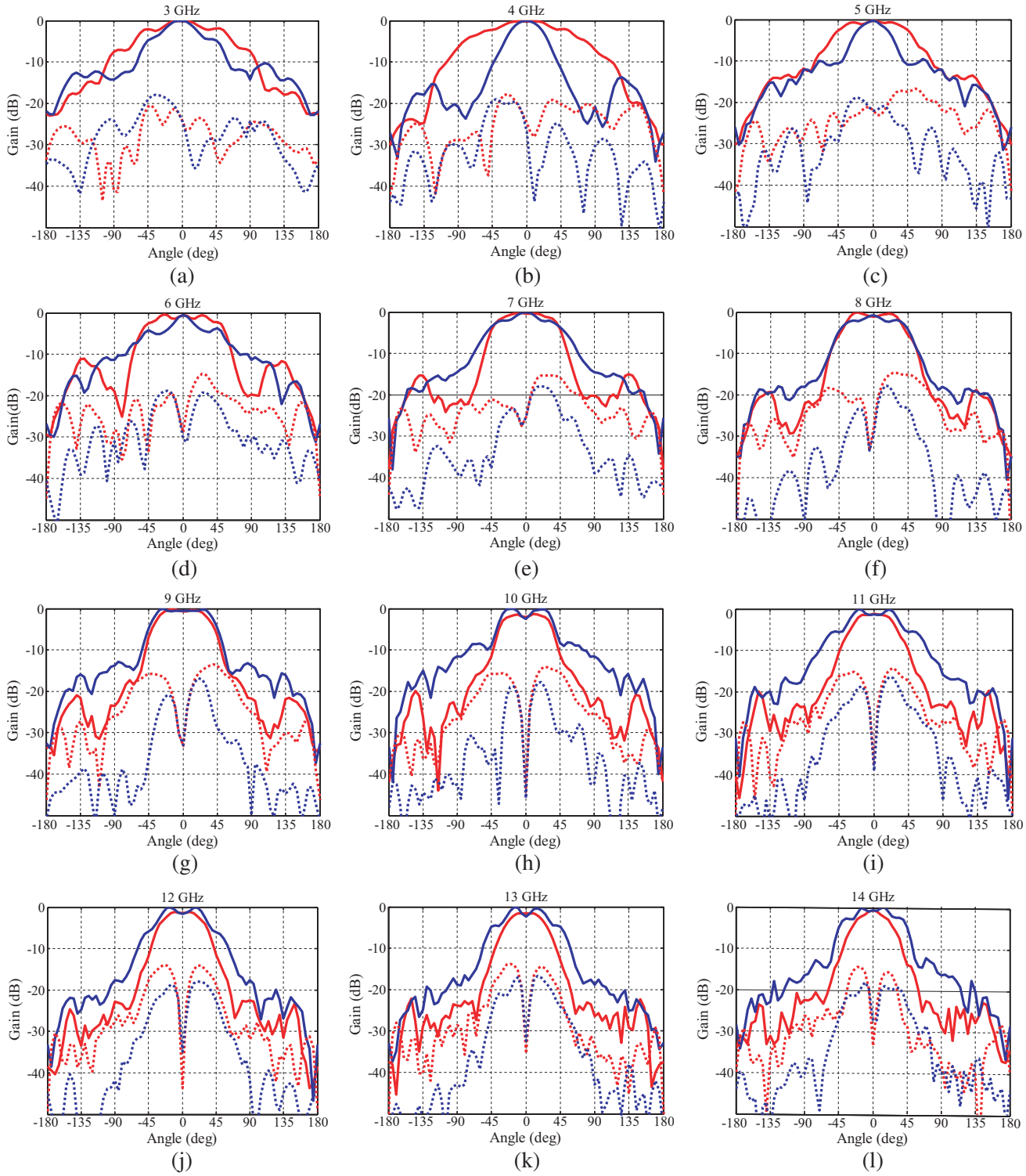

Figure 8. Measured AM DRHA normalized radiation pattern for several frequencies from 3 to 14 GHz. The solid red line for co-polar measurement in azimuth; the solid blue line for co-polar measurement in elevation; dashed red line for cross-polar component in azimuth; and dashed blue line for the cross-polar measured component in elevation.

5 deg. and a frequency resolution of 500 MHz. In the Fig. 8, the radiation pattern measured for several frequencies is shown. In the same figure, the cross- and co-polar components are introduced. The results obtained suggest that the AM DRHA works adequately on the operational frequency bandwidth. In the same way, the relation from cross- to co-polar components is keeping well separated assuring the antenna linearity.

5. CONCLUSION

In this work, the design, fabrication, and test of an AM DRHA are introduced. The antenna is built as a monolithic block using FDM technology and coated using silver ink. The antenna is optimized to work in UWB frequencies. The results obtained demonstrate an outstanding operational bandwidth performance of 11.5 GHz (fc 8.25 GHz) with a gain of 6 dBi; its total weight is less than 200 gr, and the total fabrication cost is less than 10 Euro per antenna with a lead time of less than a week.

ACKNOWLEDGMENT

The research leading to these results has received funding from the European Union's Seventh Framework Program (FP7/2007-2013) under grant agreement No. 313161, eVACUATE Project.

REFERENCES

1. Silva, J. S., E. B.Lima, J. R. Costa, C. A. Fernandes, and J. R. Mosig, "Tx-Rx lens-based satellite-on-the-move Ka-band antenna," *IEEE Antennas and Wireless Propagation Letters*, Vol. 14, 1408–1411, 2015.
2. Timbie, P. T., J. Grade, D. Weideb, B. Maffeid, and G. Pisano, "Stereolithographed MM-wave corrugated horn antennas," *Proceeding of the 36th International Conference on Infrared, Millimeter and Terahertz Waves (IRMMW-THz)*, 1–4, 2011.
3. Van der Vorst, M. and J. Gumpinger, "Applicability of 3D printing techniques for compact Ku-band medium/high-gain antennas," *Proceeding of the 10th European Conference on Antennas and Propagation (EuCAP)*, 1–4, 2016.
4. Bieren, A. E. Rijk, J.-Ph. Ansermet, and A. Macor, "Monolithic metal-coated plastic components for mm-wave applications," *Proceedings of the 39th International Conference on Infrared, Millimeter, and Terahertz Waves (IRMMW-THz)*, 1–2, 2014.
5. Vieira, K., S. Kristoffersen, J. Moen, K. Gjertsen, and T. Sverre, "Broadband antenna design using different 3D printing technologies and metallization processes," *Proceedings of the 10th European Conference on Antennas and Propagation (EuCAP)*, 1–5, 2016.
6. "ETS-3117 datasheet," ETS-Lindgren Corporation, Cedar Park, USA, [Available online] http://www.ets-lindgren.com/specs/3117.
7. "R&S®HF907 datasheet," Rohde & Schwarz, Munich, Germany, [Available online] https://www.rohde-schwarz.com/us/product/hf907-productstartpage_63493-7982.html.
8. Rong, Y. and K. A. Zaki, "Characteristics of generalized rectangular and circular ridge waveguides," *IEEE Transactions on Microwave Theory and Techniques*, Vol. 48, No. 2, 258–265, Feb. 2000.
9. Ghorbani, M. and K. N. Toosi, "Double ridged horn antenna designs for wideband applications," *Proceeding of 19th Iranian Conference on Electrical Engineering (ICEE)*, 1–5, 2011.
10. Tenigeer, N. Zhang, J. Qiu, P. Zhang, and Y. Zhang, "Design of a novel broadband EMC double ridged guide horn antenna," *Progress In Electromagnetics Research C*, Vol. 39, 225–236, 2013.
11. Rodriguez, V., "New broadband EMC double-ridge guide horn antenna," *RF Design Mag.*, May 2004.
12. "Makerbot Replicator+ datasheet," stratasys, [Available online] https://www.makerbot.com/replicator/.